Available online at www.sciencedirect.com
ScienceDirect
Journal of Power Sources 177 (2008) 669–675
JOURNAL OF POWER SOURCES
www.elsevier.com/locate/jpowsour

Short communication

The effect of the conditions of electrodeposition on the capacitive properties of dinitrobenzoyl-derivative polypyrrole films

Livia M.O. Ribeiro [a], Juliana Z. Auad [a], José G. Silva Júnior [a], Marcelo Navarro [b], Almir Mirapalheta [a], Carla Fonseca [c], Silmara Neves [c], Josealdo Tonholo [a], Adriana S. Ribeiro [a,d,*]

[a] *Instituto de Química e Biotecnologia, Universidade Federal de Alagoas, Campus A. C. Simões, 57072-970 Maceió-AL, Brazil*
[b] *Departamento de Química Fundamental, CCEN, Universidade Federal de Pernambuco, 50670-901 Recife-PE, Brazil*
[c] *Laboratório de Caracterização e Aplicação de Materiais, PPG ECM, Universidade São Francisco, 13251-900 Itatiba-SP Paulo, Brazil*
[d] *Campus Arapiraca, Universidade Federal de Alagoas, Rodovia AL-115 km 6.5, 57300-000 Arapiraca-AL, Brazil*

Received 9 October 2007; received in revised form 11 November 2007; accepted 12 November 2007
Available online 21 November 2007

Abstract

Films of poly[(*R*)-(−)-3-(1-pyrrolyl)propyl-*N*-(3,5-dinitrobenzoyl)-α-phenylglycinate] (polyDNBP) were deposited, using the galvanostatic method, onto indium tin oxide electrodes in the presence of the electrolytes tetrabutylammonium tetrafluoro-borate [$(C_4H_9)_4NBF_4$] or $LiClO_4$. Atomic force microscopy revealed that polyDNBP/$(C_4H_9)_4NBF_4$ films exhibited a grainy morphology with higher roughness and greater superficial area than polyDNBP/$LiClO_4$ films. Moreover, polyDNBP/$(C_4H_9)_4NBF_4$ films exhibited a higher capacitive electrochemical response when characterised in $LiClO_4$ rather than in $(C_4H_9)_4NBF_4$. Since polyDNBP films exhibit both n- and p-doping, they may have considerable potential application as electrodes in type III capacitor assemblies.

Keywords: Capacitor; Substituted polypyrrole film; Electrochemical properties; Morphology; Atomic force microscopy

1. Introduction

One of the major problem areas associated with the further development of applications in the fields of telecommunication devices (cell phones and GPS units), self-propelled robots, electric hybrid-vehicles, stand-by power systems, etc., relates to the storage of charge/electrical energy [1–4]. Until recently, batteries have been the most commonly used storage devices since they are able to store large amounts of energy in a relatively small volume and weight, and also provide suitable levels of power for most applications. Recently, however, the power requirements of many pieces of equipment have increased markedly and, in some cases, exceeded the capacity available using ordinary or standard-designed batteries [1].

The main characteristics of energy devices are: the total energy stored (Wh), the maximum power (W) attained, the estimated lifetime of the device, and the market cost. In order to be commercially viable, a storage device must present values for these parameters that are compatible with the requirements of the specific application. Alongside batteries and conventional capacitors, electrochemical capacitors (or super-capacitors) represent an alternative type of energy storage device. Generally, the energy densities of electrochemical capacitors (currently in the region of 1–5 $Wh\,kg^{-1}$) are much higher than those obtainable with conventional capacitors, but typically lower than those furnished by advanced batteries. However, compared with batteries, higher power densities (>500 $W\,kg^{-1}$) and longer working lifetimes (>10^5 cycles) have been either demonstrated with, or projected for, super-capacitors. Such advantages are achievable because no rate-determining or life-limiting phase transformations take place at the electrode–electrolyte interface in an electrochemical capacitor [5]. For these reasons, super-capacitors may be specified when high power is required and an extension of standard battery discharge time is necessary [6].

* Corresponding author at: Instituto de Química e Biotecnologia, Universidade Federal de Alagoas, Campus A. C. Simões, 57072-970 Maceió-AL, Brazil. Tel.: +55 3214 1389; fax: +55 3214 1389.
E-mail address: aribeiro@qui.ufal.br (A.S. Ribeiro).

0378-7753/$ – see front matter © 2007 Elsevier B.V. All rights reserved.
doi:10.1016/j.jpowsour.2007.11.035

Carbon (active carbon, active carbon fibre or carbon nanotubes), metal oxides (RuO_2, IrO_2) and conducting polymers (polyaniline, polypyrrole, polythiophenes and their derivatives) are widely employed in the construction of the electrodes of electrochemical capacitors [7–9]. Conducting polymers are particularly advantageous, offering high charge densities (*ca.* $500\,C\,g^{-1}$) compared with carbon electrodes and very low cost in comparison with noble metal oxides [10]. With conducting polymer electrodes, higher energy densities can be reached since charging occurs throughout the volume of the polymeric matrix and not just at a particulate surface. Moreover, polymeric electrodes allow fast doping/dedoping during the charge/discharge processes, good specific capacitance ($100–300\,F\,g^{-1}$) and (generally) facile synthesis through chemical and electrochemical processes [11].

In this context, polyaniline and polypyrrole are considered to be the most promising materials for application in supercapacitors by virtue of their excellent energy storage capacities, high conductivities, ease of synthesis and low cost in comparison with other conducting polymers [12,13]. However, a relatively poor long-term stability during cycling remains the main technological challenge to the industrial application of such polymers. Swelling or shrinkage of conducting polymers occurs because polymer doping requires the insertion or removal, respectively, of counter ions, thus causing volume changes that may lead to the degradation of the electrode during cycling. Moreover, it has been demonstrated that mechanical stress in a polymer film is directly associated with the maximum number of cycles that may be sustained by polymer-based capacitors [13].

Progress towards the practical application of conjugated organic polymers depends on an understanding of the fundamental chemical and physical processes that govern the properties of the materials. The electrical and optical properties of a conducting polymer are intrinsically linked to its structure, and may be tuned during electrochemical synthesis by varying the solvent, applied potential/current, monomer concentration, supporting electrolyte, temperature, etc. Since the ions of the supporting electrolyte play the role of dopant, and the counter ions ensure electric neutrality of the electrochemically doped polymer, the use of different salts as electrolyte can give rise to polymers with diverse mechanical, electrical and optical properties [14].

In previous studies, the synthesis and electropolymerisation of poly[(*R*)-(−)-3-(1-pyrrolyl)propyl-*N*-(3,5-dinitrobenzoyl)-α-phenylglycinate] (polyDNBP; Fig. 1) has been described [15], and its application as an electrochromic material investigated [16,17]. The materials employed in the construction of electrochromic and charge storage devices share many characteristics relating to chemical and structure requirements, physical–chemical operating mechanisms, and thin-film deposition techniques [18]. On this basis the present study was conducted with the aim of evaluating the potential application of polyDNBP films in the construction of charge storage devices.

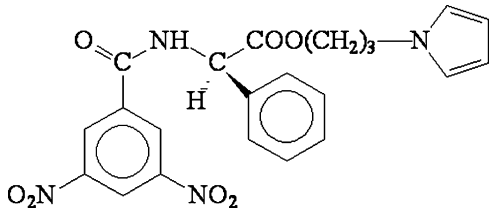

Fig. 1. Molecular structure of [(*R*)-(−)-3-(1-pyrrolyl)propyl-*N*-(3,5-dinitrobenzoyl)-α-phenylglycinate].

2. Experimental

2.1. Electrodeposition of polyDNBP films

All electrochemical experiments were performed using an Autolab (Netherlands) PGSTAT30 potentiostat equipped with a frequency response analyser module. A platinum plate was employed as the counter electrode and an $Ag/Ag^+(CH_3CN)$ home-built electrode (+0.298 V *vs.* normal hydrogen electrode; Analion, Brazil) was used as reference. DNBP monomer was synthesised and characterised as described previously [15]. Films of polyDNBP were prepared by galvanostatic deposition on indium tin oxide (ITO)/glass electrodes ($1.0\,cm^{-2}$, $Rs \leq 10\,\Omega\,cm^{-2}$; Delta Technologies, USA) at a current density (j) of $0.5\,mA\,cm^{-2}$ to produce a deposition charge (Q_{dep}) of $30\,mC\,cm^{-2}$. In these experiments, solutions containing the monomer at a concentration of $7.5 \times 10^{-3}\,mol\,L^{-1}$ in either $0.1\,mol\,L^{-1}$ $LiClO_4$ (Vetec, Brazil; used as supplied) or $0.1\,mol\,L^{-1}$ tetrabutylammonium tetrafluoro-borate [$(C_4H_9)_4NBF_4$; Merck; used as supplied] in dry acetonitrile (Omnisolv; Vetec; H_2O <0.002%, distilled over P_2O_5) were employed. After deposition, polymeric films were rinsed with CH_3CN to remove unreacted monomer and electrolyte residues.

2.2. Atomic force microscopy

Morphological characterisation of the films was carried out with the aid of a Shimadzu SPM-9500 J3 microscope, operated in the contact mode, with an Olympus Si_3N_4 cantilever probe (200 μm length). Highest quality images were obtained when a resonance frequency of 24 kHz and a spring constant of $0.15\,N\,m^{-1}$ were employed.

2.3. Electrochemical characterisation of the polyDNBP films

Films were characterised electrochemically by cyclic voltammetry, chronopotentiometry and electrochemical impedance spectroscopy (EIS) in the presence of $0.1\,mol\,L^{-1}$ $LiClO_4$ or $(C_4H_9)_4NBF_4$ in acetonitrile as electrolyte. Cyclic voltammograms were acquired within the potential scan range $-2.00 \leq E \leq 0.65\,V$ *vs.* $Ag/Ag^+(CH_3CN)$ and galvanostatic charge–discharge curves were obtained by applying a constant $j \pm 10\,\mu A\,cm^{-2}$ ($E_{cut\text{-}off} = 0.0$ and 0.5 V). All impedance spectra were recorded under open circuit potential (OCP) by applying an alternating current amplitude of 10 mV in the frequency range 10^5 to 10^{-3} Hz.

3. Results and discussion

3.1. Morphological characterisation

The effects on the morphology of polyDNBP films deposited in the presence of the supporting electrolytes $LiClO_4$ and $(C_4H_9)_4NBF_4$ may be observed by comparing the surface images depicted in Fig. 2A and B. The generic geometries of the two films were very similar, with each being composed of globular grains, but the grain size, the root mean square (RMS) roughness and the superficial area changed markedly as a function of the electrolyte. In the presence of $LiClO_4$, the mean radii of the grains were *ca.* 40–120 nm, whilst with $(C_4H_9)_4NBF_4$ the mean grain radii were in the range 120–220 nm. The structure heights were also much greater in films produced in the presence of the quaternary ammonium salt and attained 100–200 nm, i.e. values that were *ca.* 5 times larger than those for films deposited in $LiClO_4$. Generally, films produced in $LiClO_4$ presented more compact structures for which the RMS roughness and the surface area values were somewhat lower (Table 1).

The observed film morphology may be explained by the volume difference of the two electrolytes [$(C_4H_9)_4NBF_4 > LiClO_4$] incorporated into the polymeric matrix during electropolymerisation. According to Scharifker and Hills [19], during the stage of film growth controlled by diffusion, the diffusion zones begin to overlap and replacement of material at the electrode becomes hindered. As anionic and cationic species are likely to be present near to the electrode, they may both be trapped inside the polymer matrix. It is expected that the less mobile ions would be replaced more slowly by monomer molecules and thus slow down the rate of the polymer growth. $(C_4H_9)_4N^+$ is a very large cation ($r_i = 0.513$ nm) but is poorly solvated in acetonitrile, whilst Li^+ ($r_i = 0.068$ nm), although highly solvated, has a greater mobility than the tetrabutylammonium ion. [20–22]. Furthermore, the polyDNBP molecule itself is large and presents a spatial organisation that would permit more efficient ion trapping inside the polymer.

Table 1
Values of root mean square (RMS) roughness [29] and relative surface area for polyDNBP films deposited in the presence of different electrolyte systems with $Q_{dep} = 30.0\ mC\ cm^{-2}$

Electrolyte	RMS (nm)	Relative surface area
$LiClO_4$	7.65	1.020
$(C_4H_9)_4NBF_4$	29.83	1.081

3.2. Electrochemical characterisation

In order to compare the electroactivity of polyDNBP films deposited in the presence of the two electrolytes, the polymers were placed in a three-electrode cell containing the electrolytic solution ([$(C_4H_9)_4NBF_4$] or $LiClO_4$ in CH_3CN), and cyclic voltammetric, galvanostatic charge–discharge curves and EIS data collected.

The cyclic voltammograms of polyDNBP/$LiClO_4$ and polyDNBP/$(C_4H_9)_4NBF_4$ films, obtained at the anodic region in the primary system (i.e. deposition and characterisation of the film performed in the same electrolyte [14]) and in a secondary system (i.e. film characterised in an electrolyte salt different from that used in deposition), are shown in Fig. 3. As the doping/dedoping process of polymer films need a certain number of redox cycles to stabilize, due to the conformational changes occurring during the redox processes, the curves showed in Fig. 3 were acquired in the 10th redox cycle instead the 1st cycle where the cations and/or anions exchange process starts to occur.

The voltammograms indicate that, in the secondary system, both the anion and the cation of the electrolyte salt determine the redox properties of the film. The cation of the electrolyte appears to be the main factor in determining the energy required for the p-doping reaction of the film, i.e. the point at which potential oxidation of the film occurs. The shape of the voltammetric waves obtained in the presence of Li^+ were better defined than that in the presence of tetrabutylammonium ion, independent of the deposition conditions, and showed anodic and cathodic peaks separated by 90 mV suggesting reversibility of the system.

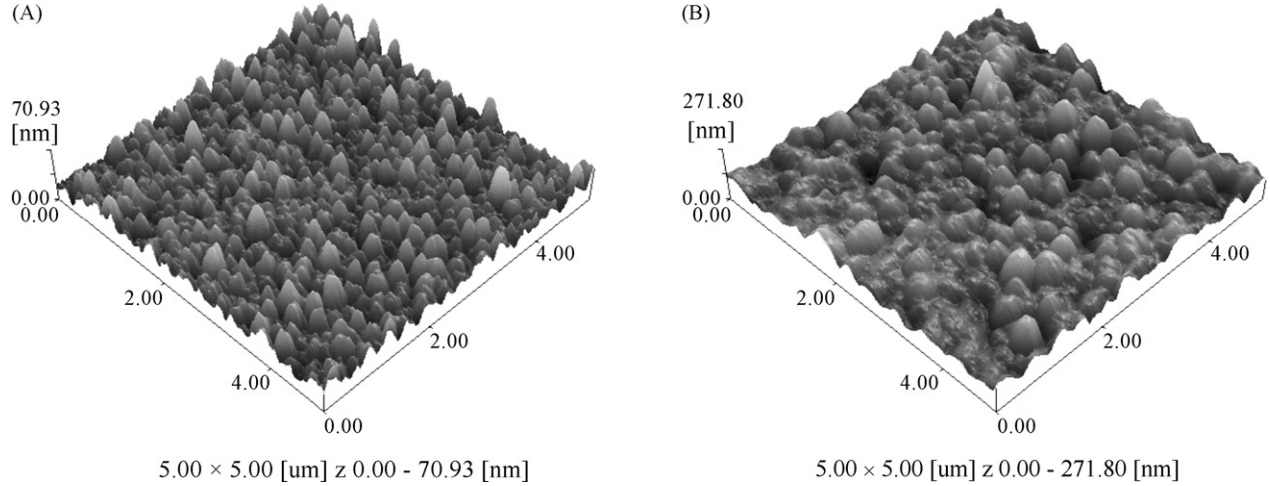

Fig. 2. Two-dimensional atomic force microscopic images, obtained in the contact mode, of polyDNBP films deposited on ITO electrode with $Q_{dep} = 30.0\ mC\ cm^{-2}$ in: (A) $LiClO_4$/acetonitrile electrolyte and (B) $(C_4H_9)_4NBF_4$/acetonitrile electrolyte.

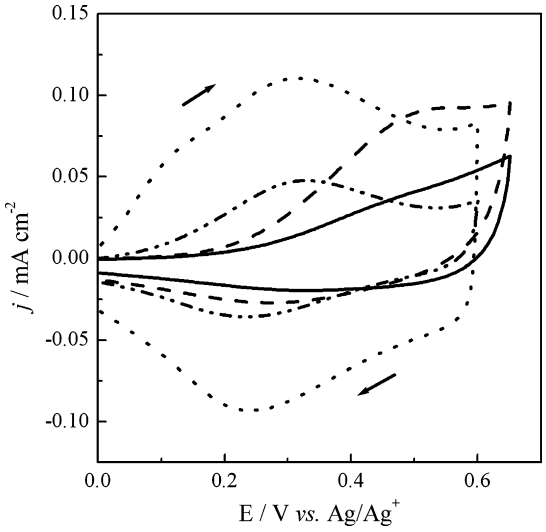

Fig. 3. Cyclic voltammograms (10th cycle) of polyDNBP films deposited on ITO electrode with $Q_{dep} = 30.0\,mC\,cm^{-2}$ in the presence of the primary electrolyte salt and characterised in primary and secondary electrolyte solutions at $\nu = 20\,mV\,s^{-1}$ showing: (—) polyDNBP/$LiClO_4$ film characterised in $(C_4H_9)_4NBF_4$, (- - - -) polyDNBP/$(C_4H_9)_4NBF_4$ film characterised in $(C_4H_9)_4NBF_4$, (-···-) polyDNBP/$LiClO_4$ film characterised in $LiClO_4$ and (· · ·) polyDNBP/$(C_4H_9)_4NBF_4$ film characterised in $LiClO_4$.

In the anodic region (p-doping), plots of peak current density (I_p) *vs.* the square root of the potential sweep rate ($\nu^{1/2}$) of films characterised in $LiClO_4$ were linear and passed through the origin, indicating a reversible behaviour, only at low sweep rate (below $35\,mV\,s^{-1}$). For scan rates above $35\,mV\,s^{-1}$, it was observed a deviation in this curve, as exemplified for the system $LiClO_4$/$LiClO_4$ shown in Fig. 4. This behaviour can be related to the ions diffusion process inside the polymer matrix [23]. The waves obtained in the presence of tetrabutylammonium ion were also independent of the deposition conditions and displayed an anodic shoulder at *ca*. 0.5 V *vs.* Ag/Ag^+ and a very weak cathodic peak, suggesting an irreversible behaviour. At the

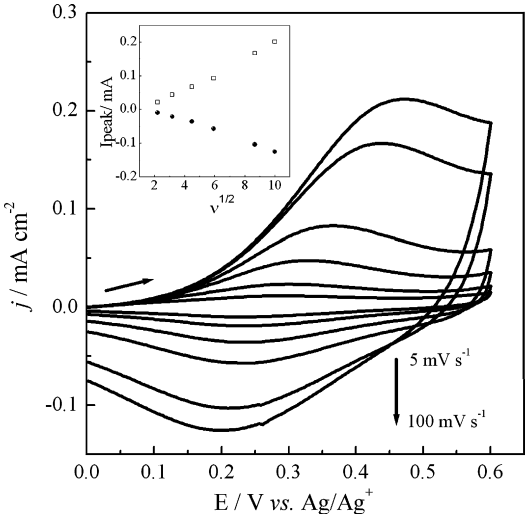

Fig. 4. Cyclic voltammogram of polyDNBP film deposited on ITO electrode with $Q_{dep} = 30.0\,mC\,cm^{-2}$ in the presence of $LiClO_4$ and characterised in $LiClO_4$ at different scan rates. The inset shows a plot of the dependence of the peak current density on the square root of the potential sweep rate.

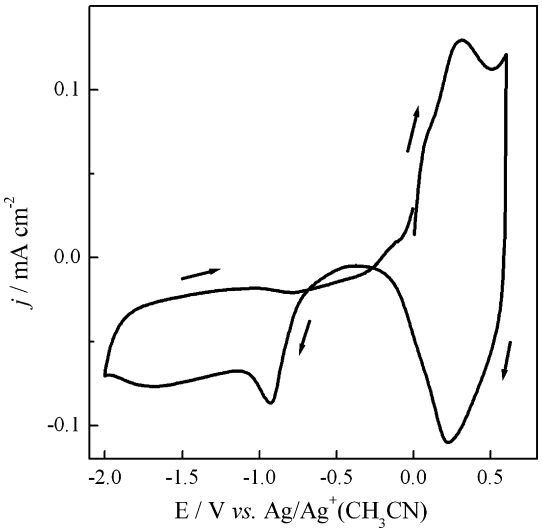

Fig. 5. Cyclic voltammogram (1st cycle) of polyDNBP film deposited on ITO electrode with $Q_{dep} = 30.0\,mC\,cm^{-2}$ in the presence of $(C_4H_9)_4NBF_4$ and characterised in $LiClO_4$ with $\nu = 20\,mV\,s^{-1}$ (scan direction $0.00 \rightarrow 0.60 \rightarrow -2.00 \rightarrow 0.00$ V *vs.* Ag/Ag^+).

cathodic region (n-doping), irreversible behaviour was observed (Fig. 5) independent of the electrolytic system employed.

The results obtained clarify the effects of the cation on both polymer film deposition (the bigger the cation the greater the surface area, voltammetric current and charge) and its characteristics in the charge–discharge process (*cf.* with $(C_4H_9)_4N^+$, Li^+ displaces the redox pair to a less anodic potential). The first of these phenomena is linked to kinetic and the second to thermodynamic parameters. It is widely accepted that the morphological characteristics of a film, some of which may be attributable to the electrolyte salt used in deposition, determine the diffusion kinetics and the rate of the doping reactions [14]. The doping process can be represented either by the insertion of anions or by the exclusion of cations from the polymer matrix. In the first case, the oxidation process could be favoured by the co-insertion of solvent molecules together with the Li^+ ion, resulting in increased swelling of the polymer and allowing easier access of doping anions. In the second case, the higher mobility of the Li^+ ion leaving the polymer could explain the differences in oxidation potentials between films cycling in Li^+ and in tetrabutylammonium electrolytes [24].

The total charge involved in the p-doping process of films deposited in the presence of $(C_4H_9)_4NBF_4$ was, in general, larger than that of those prepared in $LiClO_4$, and attained the highest level for such films when $LiClO_4$ was used as the secondary electrolytic system (Table 2). The size of the dopant anion has been reported to affect the oxidation kinetics of poly(3-methylthiophene) films [24,25]. With respect to the present study, although BF_4^- and ClO_4^- anions have similar ionic radii, the cations Li^+ and $(C_4H_9)_4N^+$ would also participate in the doping process, particularly in films prepared using $(C_4H_9)_4NBF_4$, through the action of trapping of the large ions. It appears, therefore, that the cation used in the deposition of polyDNBP has a higher impact on the electrochemical behaviour of the film so-formed than does the anionic species present.

Table 2
Electrochemical parameters determined at at $\nu = 20\,mV\,s^{-1}$ for polyDNBP films deposited and characterised in different electrolytes

Electrolyte salt used in		E_{pa} (V)	E_{pc} (V)	ΔE_p (V)	Q_{an} (mC cm^{-2})	Q_{cat} (mC cm^{-2})
Synthesis	Characterisation					
$LiClO_4$	$(C_4H_9)_4NBF_4$	0.52	0.30	0.22	0.75	0.45
$(C_4H_9)_4NBF_4$	$(C_4H_9)_4NBF_4$	0.51	0.27	0.24	1.53	0.54
$LiClO_4$	$LiClO_4$	0.33	0.24	0.09	0.88	0.64
$(C_4H_9)_4NBF_4$	$LiClO_4$	0.34	0.25	0.09	2.41	1.92

Having demonstrated that pre-formed films showed a better electrochemical response in the presence of $LiClO_4$ as electrolyte (see Fig. 3), this medium was selected for use in subsequent charge–discharge experiments performed in order to establish the deposition conditions required to optimise the electrochemical performance of the electrode as a capacitor. The charge–discharge capacitance (C) was evaluated from the linear part of the discharge curve by the relationship $C = i\,\Delta t/\Delta V$, where i is the constant current and Δt is the time interval associated with the change in voltage ΔV. The Coulombic efficiency (η) was calculated with the same current used for charging and discharging from $\eta = (t_D/t_C) \times 100\%$ where t_D and t_C are the times for discharging and charging, respectively.

Plots of the variation in charge–discharge specific capacitance as a function of cycle number are displayed in Fig. 6 for polyDNBP films deposited in $(C_4H_9)_4NBF_4$ or $LiClO_4$ and characterised in $LiClO_4$. In these experiments, specific capacitance was calculated on the basis of the mass of active material participating in the electrochemical reaction, which was determined from the surface concentration of electroactive sites (Γ) to be *ca.* 70.3 μg. During the initial cycles, polyDNBP/$(C_4H_9)_4NBF_4$ film characterised in $LiClO_4$ delivered a specific capacitance of 102 F g^{-1}, whilst polyDNBP/$LiClO_4$ film characterised in $LiClO_4$ delivered 15.8 F g^{-1}. The difference in specific capacitance values is most likely related to the larger spacing between the polymeric chains in the polyDNBP/$(C_4H_9)_4NBF_4$ film, occasioned by the voluminous $(C_4H_9)_4NBF_4$ dopant trapped in the polymer matrix during electrodeposition, which facilitates entry/exit of Li^+ ions during characterisation. The Coulombic efficiency of both films over 1–75 cycles was between 90 and 100%. The complete charging time for each cycle, however, varied from 220 to 160 s for the polymer prepared with $(C_4H_9)_4NBF_4$ and 130–90 s for the polymer prepared with $LiClO_4$.

Besides, from Fig. 6, some considerations about the stability of these films to repeated redox cycles can be made. PolyDNBP/$(C_4H_9)_4NBF_4$ film characterised in $LiClO_4$ electrolyte shows the greatest decline in capacitance with cycling (declining by 30% in only 75 cycles). This result indicates that the experimental conditions of preparation of polyDNBP films need to be improved: changing the ITO cleanning treatment, or the current density (j) used for the electrodeposition or by the modification of the substituent group (using 3,5-dinitrobenzoylglycinate instead 3,5-dinitrobenzoyl-α-phenylglycinate, for example).

Since the polyDNBP/$(C_4H_9)_4NBF_4$ film characterised in $LiClO_4$ exhibited the best capacitive properties, EIS under open circuit potential ($E = 0.100$ V *vs.* Ag/Ag$^+$; pristine electrode) were measured for this system within the range 10^{-3} to 10^5 Hz with $\Delta E = 10$ mV. The spectra presented in Fig. 7 show the

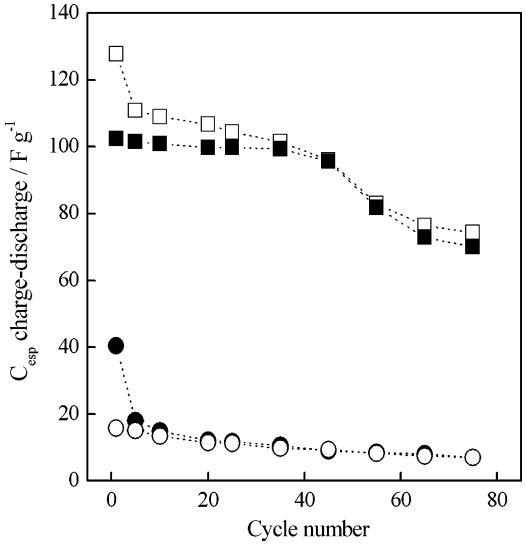

Fig. 6. Specific charge–discharge capacitance of polyDNBP films as a function of cycle number. Charge (□) and discharge (■) for polyDNBP/$(C_4H_9)_4NBF_4$ film characterised in $LiClO_4$, and charge (○) and discharge (●) for polyDNBP/$LiClO_4$ film characterised in $LiClO_4$.

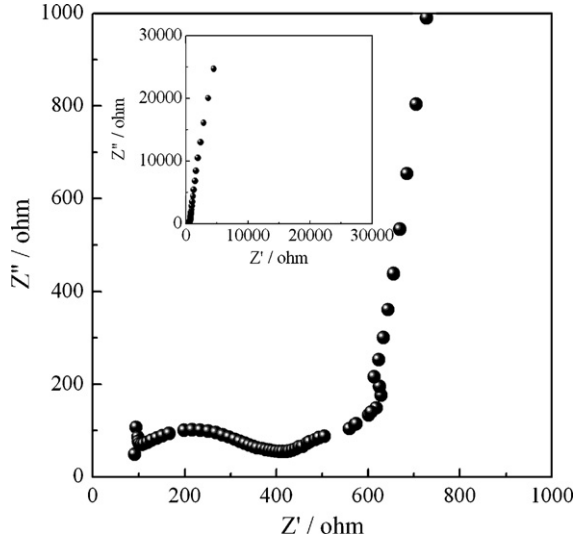

Fig. 7. Nyquist diagram of polyDNBP film deposited on ITO electrode with $Q_{dep} = 30.0$ mC cm^{-2} in the presence of $(C_4H_9)_4NBF_4$ and characterised in $LiClO_4$ at OCP.

high and medium (inset) frequency regions that are generally attributed to the double layer charging process and also to the charge transfer step. In the low frequency region, the main curve revealed a quasi-linear behaviour that is attributable to diffusional processes, which are very common in porous surfaces that are susceptible to ion movement and some capacity character.

The equations of the redox film impedance theory were used to calculate the parameters from the impedance data [26,27]. In this theory, the high frequency region identifies the electrolytic properties whilst in the mid-frequency region the impedance response is associated with the electrode/electrolyte interface. The corresponding relaxation effect is represented by a semicircle, the intersections of which with the real axis (Z') at high and mid frequencies yield the electrolytic and charge transfer resistances (R_e and R_{ct}), respectively; the time constant is the product of charge transfer resistance and double layer capacitance (C_{dl}). In the low frequency region, the impedance is controlled by the diffusion of counterions inside the composite electrode: the impedance response, ideally a 45° straight line (Warburg impedance), represents the mass transfer parameters of the electrochemical doping process. At very low frequency, when the diffusion layer involves the entire electrode thickness, the response (ideally a 90° straight line) resembles that of a pure capacitance.

Parameters R_{ct} and C_{dl} of the presumed RC-elements were obtained from the semicircles, assuming that R_{ct} was the semicircle diameter and that C_{dl} satisfied the equation $C_{dl} = (2\pi R_{ct} f_{max})^{-1}$, where f_{max} was the frequency (Hz) corresponding to the maximum value of imaginary impedance (Z'') at that semicircle [28]. The capacitive behaviour of the impedance spectra is seen in the low frequency region, i.e., the film impedance is determined by charging the film under the conditions of finite diffusion of charge carriers. The limit capacitance (C_l) can be calculated from the slope $-dZ''/d(f^{-1}) = 1/2\pi C_l$ and corresponds to the so-called redox capacity; this value is determined by the charge consumed for full oxidation/reduction of the redox sites of a polymer film. The chemical diffusion coefficient (D) can be estimate through to the plot frequency dependency of imaginary part using $\omega = 2D/h^2$ where ω is transition angular velocity and h is film thickness (30–100 nm, according AFM mapping).

From these analyses the values obtained were 71.5 and 351.1 $\Omega\,cm^{-2}$ to electrolyte and charge transfer resistances, respectively. The double layer capacitance determined was 0.4 $\mu F\,cm^{-2}$. By the other hand, the limit capacitance of poly(DNBP) film deposited in $(C_4H_9)_4NBF_4$ and characterised in $LiClO_4$ was 0.17 $F\,cm^{-2}$. The chemical diffusion coefficient was estimate $D = 3.97 \times 10^{-13}\,cm^2\,s^{-1}$.

4. Conclusions

Both the anion and the cation present in the electrolytic media employed in the polymerisation of polyDNBP films affect the structure and the electrochemical characteristics of the film so-formed. Moreover, since both ionic species are trapped in the polymer matrix during film formation, a change in the supporting electrolyte in the ensuing redox studies may give rise to an alteration in the electrochemical properties of the polymer.

The deposition of polyDNBP films in the presence of $(C4H9)_4NBF_4$ and subsequent characterisation in the presence of $LiClO_4$ provided the best electrolytic conditions for charging the polymeric film. This finding can be attributed to the greater surface area obtained through the use of a large molecule $[(C_4H_9)_4NBF_4]$ as electrolyte, thereby providing parallel ionic and electronic conduction pathways that facilitate the process of charge transfer and mass transport.

Since polyDNBP films display both n- and p-doping, their capacitive properties are appropriate for a type III capacitor assembly. Furthermore, considering the EIS results and the film thickness (30–100 nm according atomic force microscopic mapping), the capacitance of polyDNBP films may attain 60–200 $C\,cm^{-3}$, a value that is a very promising with respect to the development of technological applications.

Acknowledgements

The authors wish to thank the granting authorities CNPq, FINEP, FAPESP and FAPEAL for financial support and for fellowships to A.M. and J.G.S.J. (CAPES), J.Z.A. and L.M.O.R. (FAPEAL). Thanks are also due to Braskem Co. (Brazil) for partnership in technological development.

References

[1] A. Burke, J. Power Sources 91 (2000) 37.
[2] R. Kotz, M. Carlen, Electrochim. Acta 45 (2000) 2483.
[3] S. Sarangapani, B.V. Tilak, C.-P. Chen, J. Electrochem. Soc. 143 (1996) 3791.
[4] S.A. Hashmi, A. Kumar, S.K. Tripathi, Eur. Polym. J. 41 (2005) 1373.
[5] A. Rudge, J. Davey, I. Raistrick, S. Gottesfeld, J.P. Ferraris, J. Power Sources 47 (1994) 89.
[6] J.-W. Sung, S.-J. Kim, K.-H. Lee, J. Power Sources 124 (2003) 343.
[7] J.P. Zheng, J. Huang, T.R. Jow, J. Electrochem. Soc. 144 (1997) 2026.
[8] J.P. Zheng, T.R. Jow, J. Electrochem. Soc. 142 (1995) 2699.
[9] S. Panero, E. Spila, B. Scrosati, J. Electroanal. Chem. 396 (1995) 385.
[10] S.A. Hashmi, H.M. Upadhyaya, Solid State Ionics 152 (2002) 883.
[11] J.-H. Sung, S.-J. Kim, K.-H. Lee, J. Power Sources 133 (2004) 312.
[12] S. Gottesfeld, A. Redondo, S.W. Feldberg, J. Electrochem. Soc. 134 (1994) 271.
[13] V. Khomenko, E. Frackowiak, F. Beguin, Electrochim. Acta 50 (2005) 2499.
[14] R.-M. Latonen, C. Kvarnström, M. Grzeszczuk, A. Ivaska, Synth. Met. 130 (2002) 257.
[15] A.S. Ribeiro, A. Kanazawa, D.M.A.F. Navarro, J.-C. Moutet, M. Navarro, Tetrahedron: Asymmetry 10 (1999) 3735.
[16] A.S. Ribeiro, A.U. da Silva, L.M.O. Ribeiro, J.G. da Silva Jr., M. Navarro, J. Tonholo, J. Electroanal. Chem. 580 (2005) 313.
[17] A.S. Ribeiro, A.U. da Silva, M. Navarro, J. Tonholo, Electrochim. Acta 51 (2006) 4892.
[18] K.-H. Heckner, A. Kraft, Solid State Ionics 152 (2002) 899.
[19] B. Scharifker, G. Hills, Electrochim. Acta 28 (1983) 879.
[20] M. Salomon, E.J. Plichta, Electrochim. Acta 29 (1984) 731.
[21] V. Carlier, M. Skompska, C. Buess-Herman, J. Electroanal. Chem. 456 (1998) 139.
[22] V. Peulon, G. Barbey, J.-J. Malandain, Synth. Met. 82 (1996) 111.

[23] W.A. Gazotti, R. Faez, M.-A. De Paoli, J. Electroanal. Chem. 415 (1996) 107.
[24] P. Marque, J. Roncali, F. Garnier, J. Electroanal. Chem. 218 (1987) 107.
[25] F.-J. Pern, A. Frank, J. Electrochem. Soc. 137 (1990) 2769.
[26] M.F. Mathias, O. Haas, J. Phys. Chem. 96 (1992) 3174.
[27] E.G. Tolstopyatova, S.N. Sazonovo, V.V. Malev, V.V. Kondratiev, Electrochim. Acta 50 (2005) 1565.
[28] N.G. Skinner, E.A.H. Hall, Synth. Met. 63 (1994) 133.
[29] L.H.C. Batista, J.G. da Silva Jr., M.F.A. Silva, J. Tonholo, Microsc. Microanal. 13 (2007) 245.